Journal of Nuclear Materials 403 (2010) 113–116

Contents lists available at ScienceDirect

Journal of Nuclear Materials

journal homepage: www.elsevier.com/locate/jnucmat

The role of minor alloying elements on the stability and dispersion of yttria nanoclusters in nanostructured ferritic alloys: An ab initio study

D. Murali, B.K. Panigrahi *, M.C. Valsakumar, Sharat Chandra, C.S. Sundar, Baldev Raj

Materials Science Group, Indira Gandhi Centre for Atomic Research, Kalpakkam 603 102, India

ARTICLE INFO

Article history:
Received 4 February 2010
Accepted 4 June 2010

ABSTRACT

Nanostructured ferritic alloys derive their strength from the dispersion of oxide nanoclusters in the ferritic matrix. We have explored the relative role of minor alloying elements like Ti and Zr on the stability of nanoclusters of vacancy–Y–Ti–O by density functional theory calculations and shown that the binding energy of these clusters increases when we replace Ti with Zr. This could imply faster nucleation of the nanoclusters which, in turn, may lead to finer dispersion of nanoclusters resulting in improved performance of ferritic alloys. Further, we show a core/shell structure for these nanoclusters in which the core is enriched in Y, O, Ti while the shell is enriched in Cr.

© 2010 Elsevier B.V. All rights reserved.

1. Introduction

Mechanically alloyed nanostructured ferritic alloys (NFA) are potential candidates for core structural applications at elevated temperatures in high energy neutron environments of fast breeder and fusion reactors [1]. NFA's are characterized by dispersion of thermally stable oxygen rich nanoclusters in the ferritic matrix. The dispersion of oxide nanoclusters is further improved by the addition of Ti resulting in the very high number density ($\sim 10^{23}$–$10^{24}/m^3$) of nanosized (~2–5 nm) oxygen rich Y–Ti–O nanoclusters [2]. The oxide nanoclusters act as obstacles to dislocation motion thereby reducing creep rate; serve as dominant nucleation sites for small helium bubbles and promote vacancy–interstitial recombination, thus exhibiting high resistance to radiation damage. These nanoclusters are observed to reduce the creep rate at 923–1173 K by six orders of magnitude and are highly stable even at elevated temperatures, with no coarsening of the nanoclusters observed even after 14,000 h creep studies at 1073 K [2]. The improved creep resistance of the material at high temperatures, compared to their conventional ferritic martensitic counterparts, increases the possible operating temperature of these materials to 923 K or higher in intense radiation environment. Recent experimental results [3] suggest that yttria particles dissolve in the ferritic matrix during the mechanical alloying process and subsequently precipitate along with Ti in the high temperature consolidation process which involves either hot extrusion or high temperature hot isostatic pressing. The presence of Ti is required for obtaining ultrafine particles with a high density [4]. This is a major benefit as precipitate dispersion in the matrix controls the creep properties. Further, a size range of 2–5 nm is required for these particles to be stable in presence of high neutron flux for their use as structural materials in advanced reactors. Atom probe tomography (APT), small angle neutron scattering and transmission electron microscopy studies have been extensively used to characterize the nanoclusters in the ferritic matrix [2–10]. The precipitate structure as well as their size and spatial distribution depend on the alloy composition and the processing parameters such as the consolidation temperature, milling conditions, etc. For example, the number density is found to decrease and the radii of nanoclusters increase with the higher consolidation temperature [3]. The metal to oxygen ratio is generally >1 for these coherent transition nanoclusters compared to incoherent complex oxide phases of $Y_2Ti_2O_7$ or Y_2TiO_5. APT analysis of ODS steels containing Ti has shown [2] that these nanoclusters contain Y, O and Ti. The depletion of Cr atoms in the nanoclusters is observed by Miller et al. [2]. Recently Marquis [10] has done detailed APT analysis of the composition of the nanoclusters in three different ODS alloys, viz., MA957, ODS Fe–12 wt.% Cr and ODS-Eurofer-97 and found that the nanoclusters have a core/shell structure. The core region of the nanocluster is enriched in O, Y, Ti and depleted in Cr. In model ODS Fe–12 wt.% Cr, the shell region is found to be enriched in Cr.

In order to gain knowledge about the structure and stability of these nanoclusters in the ferritic matrix, we have done detailed first principles calculations. The sizes and complexity of the nanoclusters themselves are far beyond the direct capability of such calculations. However, basic energetic properties of the solutes and the earliest stages of solute clustering are needed to understand the larger nanocluster structure and compositions as well as their long term stability at elevated temperatures. The density functional theory calculations of Fu et al. [11] and the positron annihilation experimental studies [12] reveal that vacancies

* Corresponding author. Tel./fax: +91 (44) 27480081.
E-mail address: bkp@igcar.gov.in (B.K. Panigrahi).

0022-3115/$ - see front matter © 2010 Elsevier B.V. All rights reserved.
doi:10.1016/j.jnucmat.2010.06.008

constitute an essential ingredient in the nanocluster formation. However, the DFT calculations of Jiang et al. [13] show that the solute clustering can take place without the energetic assistance of pre-existing vacancies in the Fe matrix.

In this paper, we have calculated the formation and binding energies of clusters of O, Y, vacancy (V), Cr along with Ti or Zr in bcc iron matrix in order to explore the role of the minor alloying elements [14] like Ti and Zr on the stability and dispersion of nanoclusters. We have shown that the binding energy of the various Y–V–O clusters increases with the addition of Ti or Zr and the increase in binding energies is more for Zr which, in turn, can lead to higher stability. The higher stability for these clusters can contribute to the faster nucleation rate which in turn can influence the size and number density of the nanoclusters. Further, considering the interaction of Cr with O, Y, vacancy and Ti and their clusters, we show a core/shell structure for these nanoclusters in which the core is enriched in Y, O, Ti (Zr) while the *shell* is enriched in Cr.

2. Details of the calculation

We have performed our calculations using the Vienna ab initio simulation package (VASP) within the density functional theory [15]. All the calculations were performed in a plane wave basis, using pseudopotentials generated within the projected augmented wave (PAW) approach [16]. For the calculations of transition metals and magnetic systems, PAW method is generally preferred compared with the ultra-soft pseudopotential approach [17]. All the calculations were done using the spin polarized formalism and within the generalized gradient approximation [18]. Supercell approach and periodic boundary conditions were used for the calculations of the perfect system as well as systems containing defect species. Convergence tests were carried out for both Brillouin zone sampling and plane wave energy cutoff until energies converged to 0.1 meV per atom. All the calculations were done with a 128-atom supercell and Brillouin zone sampling was performed using the Monkhorst and Pack scheme [19]. We have used $2 \times 2 \times 2$ k grid for the Brillouin zone sampling and 500 eV for the plane wave energy cutoff. For the larger defect cluster calculations, we have used the 250 atom supercell with $1 \times 1 \times 1$ k grid for the Brillouin zone sampling and 500 eV for the plane wave energy cutoff.

The formation energies in bcc Fe were calculated using the following relation [13]

$$E_{\text{form}} = E_{\text{D}} - E_0 - \mu_{\text{Fe}}\Delta n_{\text{Fe}} - \mu_{\text{X}}\Delta n_{\text{X}}, \quad (1)$$

where E_{D} and E_0 denote the energies of the supercell with and without defects, and μ_{X} and Δn_{X} are the chemical potential of species X and the difference in number of atoms of type X between the two supercells. The chemical potentials of Y, Ti and Zr were calculated with respect to the equilibrium hcp phases, respectively.

The binding energy between two defect species (A_1 and A_2) in bcc iron matrix is calculated as follows [20]

$$E_{\text{b}}(A_1, A_2) = [E(A_1 + A_2) + E_{\text{ref}}] - [E(A_1) + E(A_2)], \quad (2)$$

where E_{ref} is the energy of the supercell without any defect. $E(A_1)$ is the energy of the supercell with defect A_1 and $E(A_2)$ is the energy of the supercell with defect A_2. $E(A_1 + A_2)$ is the energy of the supercell with A_1 and A_2 interacting with each other. For more than two interacting defect species the above equation can be generalized as follows

$$E_{\text{b}}(A_1, \cdots, A_n) = [(n-1)E_{\text{ref}} + E(A_1 + \cdots + A_n)] - \left[\sum_1^n E(A_i)\right], \quad (3)$$

A positive binding energy means attraction between the defects and negative binding energy means repulsion between them. This definition is used to calculate the binding energies of the defect clusters in our present study.

3. Results and discussion

In the following sections we have presented and discussed the basic energetic properties of Y, Ti, O, Cr and their clusters in the presence of vacancy in bcc Fe. Our calculations indicate that the stable configuration for the O atom is octahedral position whereas the stable positions for Y, Ti and Cr atoms are substitutional positions. The formation energies of O in octahedral, tetrahedral and substitutional position are 1.35 eV, 1.76 eV, and 3.01 eV, respectively, indicating octahedral site as the preferred site for O. The formation energy of Y in substitutional position in bcc Fe is found to be 1.86 eV. The very high formation energies of Y and O atom in bcc Fe indicate the very low solubility of these elements in bcc Fe which agrees with the calculations of Fu et al. [11]. In contrast to the repulsive interaction of Y and O with Fe, high attractive interaction of Ti and Cr with Fe is indicated from the calculated formation energies of −0.8 eV and −0.3 eV, respectively.

Next, we have calculated the binding energy of Y, Ti, O and Cr with vacancy as supersaturation of vacancies is produced in the milling process [21–24] and the vacancy concentration increases by about 15 orders of magnitude in the mechanical alloying of Fe–Cu system [23]. The binding energies of Y, Ti, O and Cr with vacancy are presented in Table 1. The binding of oxygen atom in octahedral position with vacancy is found to be very high value of 1.65 eV which effectively decreases the formation energy of oxygen in Fe matrix. Thus, high concentration of vacancies produced in the mechanical alloying process can act as trapping centers for the oxygen atoms thereby producing O–V pairs. The binding energy of Y atom with vacancy in the first neighbor position is found to be 1.45 eV and in the second neighbor position is 0.25 eV. The appreciable binding of Y atom with second neighbor vacancy is due to the large size of Y atom in Fe matrix. The relaxation of Fe atoms around the Y is found to be very high and also when vacancy is created first neighbor to Y atom, it relaxes 0.76 Å towards the vacancy, thereby forms strong interaction with vacancy. In contrast

Table 1
The binding energies of the Y, Ti, O and Cr and their clusters in bcc Fe. We have considered oxygen in octahedral interstitial position and Y, Ti and Cr atoms were in substitutional positions and pairs of clusters in first (1NN) and second-nearest neighbor (2NN) distances in bcc Fe. For the pair interaction energies of Y, Ti, Cr and vacancy (V), 1NN and 2NN corresponds to distances of $\sqrt{3}/2\mathbf{a}$ and $\mathbf{a}$, respectively, whereas for oxygen atom interaction with Y, Ti, Cr and vacancy (V), 1NN and 2NN corresponds to distances of $\mathbf{a}/2$ and $\mathbf{a}/\sqrt{2}$, respectively. Here, the value of $\mathbf{a}$ is 2.83 Å. A positive binding energy indicates a total-energy reduction resulting from an energy-favored cluster formation. The references values in the parentheses correspond to first and second neighbor distances.

Defect configuration	Binding energy (eV)		
	1NN	2NN	References
O–V	1.65	0.75	(1.55[a], 0.75[b])
Y–V	1.45	0.26	
Ti–V	0.26	0.16	(0.30[A,c])
Cr–V	0.05	0.02	(0.10[A,d])
Y–O	−0.35	1.01	(−0.24[a], 1.00[a])
Ti–O	0.26	0.55	(0.24[a], 0.50[a])
Cr–O	0.25	−0.02	
Cr–Cr	−0.21	−0.13	
Cr–Y	−0.16	−0.15	
Cr–Ti	−0.15	−0.11	

[A] Experiment.
[a] Ref. [13].
[b] Ref. [11].
[c] Ref. [25].
[d] Ref. [26].

to Y and O atoms, Ti atom is found to have less binding with vacancy which is in agreement with the positron annihilation studies of Triftshäuser et al. [25]. A small repulsion is observed for Ti–V pair in the second neighbor position. The Cr–vacancy binding is very small in the first neighbor position in agreement with the muon spectroscopy results [26]. Compared to the very high binding of O–V and Y–V defect cluster, Cr is found to have negligible interaction with vacancy.

Now, we consider the role of vacancies in the nanocluster formation in bcc Fe by calculating the binding energies of solute vacancy complexes. The change in energy when Y, Ti, O or Cr is added to the Fe matrix containing different defect clusters is presented in Fig. 1. From the figure, it is clear that Y and O atoms in bcc Fe gain substantial energy when vacancy is present in the matrix suggesting the crucial role of vacancies in the nanocluster formation. Both Y and Ti atoms show strong affinity towards oxygen in bcc Fe when O is in the second neighbor position to Y or Ti. The change in energy when Y and Ti are added to the O atom in the Fe matrix is found to be 1.01 eV and 0.55 eV, respectively. The change in energy when Y and Ti are added to the O–V pair in the Fe matrix is found to be 1.65 eV and 0.8 eV, respectively. Consequently the binding energies of energy optimized configuration of Ti–O–V and Y–V–O cluster is found to be a very high value of 2.45 and 3.35 eV, respectively. Y and O atoms relaxes considerably in the Y–V–O cluster resulting in the strong bonding between Y and O atoms. This high binding energy of Y–V–O clusters plays an important role in the structure and exceptionally high stability of the nanoclusters. When we add Ti to the Y–V–O cluster, the binding energy further increases to 4.1 eV. We have also calculated the binding energies of a few of the larger Y–Ti–O clusters with vacancies by taking the APT composition of nanoclusters obtained by Marquis [10]. The binding energy of $Y_2O_4V_2$ cluster is 8.7 eV. A further addition of four Ti atoms to this cluster increases the binding energy to as high as 12.5 eV. This exceptionally high binding energy will make these clusters ultrastable and the cluster could act as nucleation sites for the growth of the nanoclusters [3] and the presence of Ti in the periphery, as indicated by the attractive interaction of Fe with Ti (see Fig. 1) and higher binding energy for Ti containing clusters, could reduce the interfacial energy resulting in higher number density of the nanoclusters.

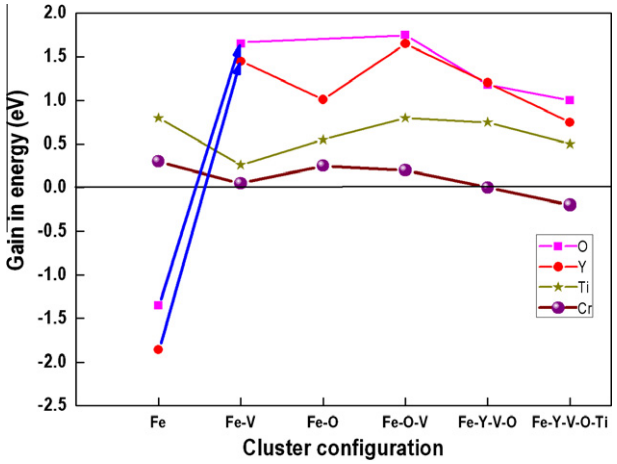

Fig. 1. The gain in energy when Y, Ti, O or Cr is added to the Fe matrix and Fe matrix containing vacancy (V), O, O–V, Y–V–O and Y–V–O–Ti defect clusters. Positive energy means attractive interaction between Y, Ti, O and Cr with matrix or defect clusters in the matrix. Please note that the binding energies of Cr atom interactions with the vacancy and the defect clusters is negligible compared with the Y, O and Ti interactions. Blue arrows indicate the high gain in energy for O and Y in the presence of vacancy. (For interpretation of the references to colour in this figure legend, the reader is referred to the web version of this article.)

Now we consider the interaction of Cr atom with Y, Ti, O and their clusters in bcc Fe. The binding energies of Cr–Cr, Cr–Y, Cr–Ti and Cr–O in bcc Fe in the first and second neighbor positions were calculated and presented in Table 1. The positive binding energies of Cr with Y and Ti suggest that they interact repulsively in bcc Fe. The repulsion is stronger even in the second neighbor distance and becomes negligible in the third neighbor distance. Since core of the nanocluster contain Y and Ti atoms, the repulsive interaction of Cr with Y and Ti would suggest depletion of Cr in the core of the nanoclusters. Also, the vacancy formation energy in bcc Cr is 0.5 eV higher than the vacancy formation energy in bcc Fe which suggest the presence of Cr in the nanoclusters is not favored through vacancy mechanism. From the Fig. 1, it is clear that the Cr atom is having negligible interaction with vacancy, O–V, Y–V–O and repulsive interaction with the Y–V–O–Ti cluster which suggests that the energetics of cluster formation least favors the presence of Cr atom in the nanoclusters. These energetic trends suggest a core/shell structure for these nanoclusters in which the core is enriched in Y, O, Ti while the shell is enriched in Cr as observed by Marquis [10].

We have explored usage of other similar alloying elements like Zr in place of Ti in the nanocluster formation in bcc Fe. The formation energies of Ti and Zr in bcc Fe is −0.8 eV and 0.16 eV, respectively. In order to better understand the bonding characteristics, we have done the differential charge density distribution of substitutional Ti and Zr in bcc Fe and the results are shown in Fig. 2. From the figure it is clear that the Zr atom losses charge to the interstitial regions resulting in the weak Zr–Fe bond compared with the strong

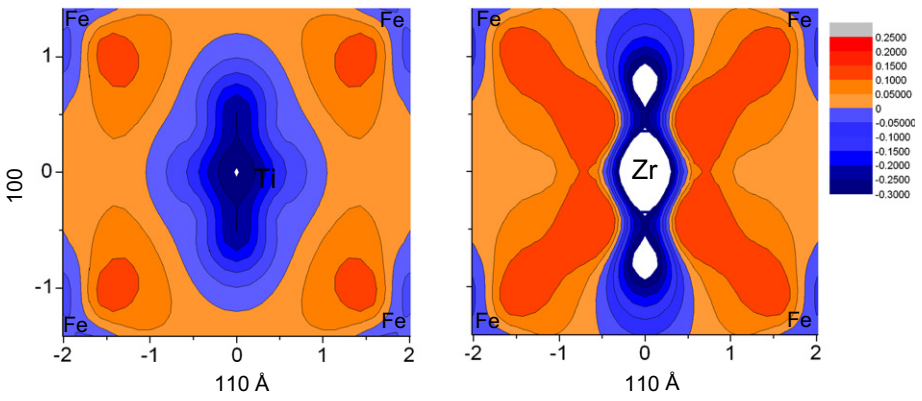

Fig. 2. The differential charge density map of substitutional Ti (left) and Zr in 128 atom bcc Fe supercell. The charge distributions are expressed in the units of electrons/Å^3 in (1 1 0) plane. The charge density of the white regions are below −0.3 electrons/Å^3.

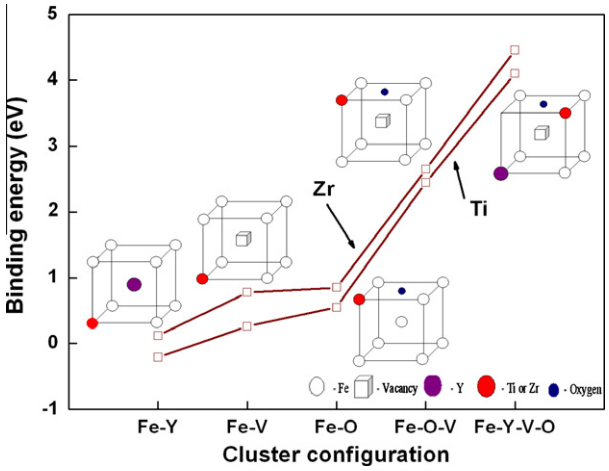

Fig. 3. The binding energies of Ti and Zr atoms with vacancy (V), O, O–V and Y–V–O cluster in bcc Fe supercell. The schematic of the atom positions in the energy optimized defect clusters is shown inside the figure. Here, the empty circles represents the Fe atoms, the cube represents the vacancy, the pink circle represents the Y atom, red circles represents the Ti or Zr atom and blue circle represent the O atom. (For interpretation of the references to colour in this figure legend, the reader is referred to the web version of this article.)

directional bond for the Ti atom with nearest neighbor Fe atoms. The bonding characteristics are in agreement with their formation energy trends. We have calculated the binding energies of Zr with Y, O, V and their clusters in bcc Fe (Ti is replaced with Zr in the defect cluster) and the results of the energy optimized configurations are presented in Fig. 3. The binding energies of Zr and Ti with Y in Fe matrix are 0.12 eV and −0.21 eV, respectively, which clearly shows that the Zr atom is having attractive interaction with Y as compared with the repulsive interaction of Ti with Y. Also from the figure, it is clear that the binding energies of O, V and their clusters are higher when we replace Ti with Zr. Further, we have performed energy minimization of Y–V–O–Ti cluster and Y–V–O–Zr clusters by varying the positions of Y and Ti or Zr with respect to O–V pair. In all the different configurations investigated, the binding energies of Y–V–O–Zr are high compared with the corresponding Y–V–O–Ti clusters suggesting very high thermal stability for these clusters. Also the bond lengths of Y–O and Zr–O in the minimum energy configuration of Y–V–O–Zr are 2.30 Å and 2.05 Å, respectively, where as the bond lengths of Y–O and Ti–O in the Y–V–O–Ti defect cluster are 2.71 Å and 2.37 Å, respectively. This reduction in the bond lengths for the defect clusters containing Zr atom is mainly due to the strong interaction of Zr with vacancy and attractive interaction between Y and Zr. These results suggest replacing Ti with Zr leads to the higher stability for the nanoclusters. This higher stability for the clusters can contribute to enhanced nucleation rate which in turn can influence the dispersion of nanoclusters [14].

4. Conclusion

Compared with the Y, Ti, O and vacancy interactions among themselves, Cr is having negligible interaction with vacancy, O, O–V and repulsive interaction with Y and Ti which suggests the core/shell structure for these nanoclusters in which core is enriched in Y, Ti, O and shell is enriched in Cr. The binding energies of the clusters increase when we replace Ti with Zr leading to the higher stability. The higher stability of these clusters can contribute to enhanced nucleation rate, which may give rise to a finer dispersion of the nanoclusters, provided the other factors such as diffusion, growth rate, etc., are conducive. The finer dispersion of the nanoclusters may result in improved performance of the ferritic alloy.

References

[1] G.R. Odette, M.J. Alinger, B.D. Wirth, Annu. Rev. Mater. Res. 38 (2008) 471.
[2] M.K. Miller, E.A. Kenik, K.F. Russell, L. Heatherly, D.T. Hoelzer, P.J. Maziasz, Mater. Sci. Eng. A 353 (2003) 140.
[3] M.J. Alinger, G.R. Odette, D.T. Hoelzer, Acta Mater. 57 (2009) 392.
[4] M. Ratti, D. Leuvrey, M.H. Mathon, J. Nucl. Mater. 386 (2009) 540–543.
[5] T. Yamamoto, G.R. Odette, P. Miao, D.T. Hoelzer, J. Bentley, N. Hashimoto, H. Tanigawa, R.J. Kurtz, J. Nucl. Mater. 367 (2007) 399.
[6] D.T. hoelzer, J. Bentley, M.A. Sokolov, M.K. Miller, G.R. Odette, M.J. Alinger, J. Nucl. Mater. 367 (2007) 166.
[7] M.K. Miller, D.T. hoelzer, E.A. Kenik, K.F. Russsell, J. Nucl. Mater. 329 (2004) 338.
[8] M.K. Miller, K.F. Russel, D.T. Hoelzer, J. Nucl. Mater. 351 (2006) 261.
[9] M.K. Miller, D.T. Hoelzer, E.A. Kenik, K.F. Russel, Intermetallics 13 (2005) 387.
[10] Emmanuelle A. Marquis, Appl. Phys. Lett. 93 (2008) 181904.
[11] C.L. Fu, Maja Krčmar, G.S. Painter, Xing-Qiu Chen, Phys. Rev. Lett. 99 (2007) 225502.
[12] Jun Xu, C.T. Liu, M.K. Miller, Hongmin Chen, Phys. Rev. B 79 (2009) 020204(R).
[13] Yong Jiang, John R. Smith, G.R. Odette, Phys. Rev. B 79 (2009) 064103.
[14] Y. Uchida, S. Ohnuki, N. Hashimoto, T. Suda, T. Nagai, T. Shibayama, K. Hamada, N. Akasaka, S. Ymashita, S. Oshstuka, T. Yoshitke, Mater. Res. Soc. Symp. Proc. 981 (2007). 0981-JJ07-09.
[15] G. Kresse, J. Furthmuller, Comput. Mater. Sci. 6 (1996) 15.
[16] G. Kresse, D. Joubert, Phys. Rev. B 59 (1999) 1758.
[17] D. Vanderbilt, Phys. Rev. Lett. 96 (2006) 175501.
[18] J.P. Perdew, Y. Wang, Phys. Rev. B 45 (1992) 13244.
[19] H.J. Monkhorst, J.D. Pack, Phys. Rev. B 13 (1976) 5188.
[20] Pär Olsson, Christophe Domain, Janne Wallenius, Phys. Rev. B 75 (2007) 014110.
[21] P. Pochet, E. Tominez, L. Chaffron, G. Martin, Phys. Rev. B 52 (1995) 4006.
[22] Jia Ye, Phys. Rev. B 70 (2004) 094104.
[23] X. Sauvage, F. Wetscher, P. Pareige, Acta Mater. 53 (2005) 2127.
[24] B.Q. Zhang, L. Lu, M.O. Lai, Physica B 325 (2003) 120.
[25] W. Triftshäuser, H. Matter, J. Winter, Appl. Phys. A 28 (1982) 179.
[26] A. Möslang, H. Graf, G. Balzer, E. Recknagel, A. Weidinger, Th. Wichert, Phys. Rev. B 27 (1983) 2674.